# Secure Euclidean random distribution for patients' magnetic resonance imaging privacy protection

**Ali Jaber Tayh Albderi, Lamjed Ben Said**
Department of SMART Laboratory, University of Tunis, ISG, Tunisia

**Article Info**

***Article history:***

Received Feb 10, 2023
Revised Sep 23, 2023
Accepted Oct 14, 2023

***Keywords:***

Euclidean distribution
Image steganography
Least signification bit
Most signification bit
Patients' magnetic resonance imaging privacy

**ABSTRACT**

Patients' information and images transfer among medical institutes represent a major tool for delivering better healthcare services. However, privacy and security for healthcare information are big challenges in telemedicine. Evidently, even a small change in patients' information might lead to wrong diagnosis. This paper suggests a new model for hiding patient information inside magnetic resonance imaging (MRI) cover image based on Euclidean distribution. Both least signification bit (LSB) and most signification bit (MSB) techniques are implemented for the physical hiding. A new method is proposed with a very high level of security information based on distributing the secret text in a random way on the cover image. Experimentally, the proposed method has high peak signal to noise ratio (PSNR), structural similarity index metric (SSIM) and reduced mean square error (MSE). Finally, the obtained results are compared with approaches in the last five years and found to be better by increasing the security for patient information for telemedicine.



***Corresponding Author:***

Ali Jaber Tayh Albderi
Smart Lab, University of Tunis, ISG
41 Av. de la Liberte, Tunis 2000, Tunisia
Email: ali.jaber.tayh@gmail.com

## 1. INTRODUCTION

The fast expansion of technology over the internet has resulted in a high difficulty for managing image data by researchers, especially in text transfer in telemedicine [1]. The hiding information techniques have significant achieving security especially that are send through internet to save from hackers [2]–[4]. A dedicated and novel algorithm is required to satisfy the new equipment. Secret text still represent a common language and tool among senders and receiver [5]–[7].

With the fast growth in telemedicine applications, the communication of a patient's diagnostic medical data has become more common in the healthcare sector [8], [9]. Technically, healthcare data should be secured using potential techniques of security, which provide more protection for sensitive data from various attacks [10]–[12]. In this work, we discuss the issue of unauthorised access to medical images in order to provide high security for patient sensitive information [13], [14].

In this paper, a new security telemedicine secure random distribution for secret bits is suggested. The Euclidean mathematical distribution has been developed to support new random selections. This secure distribution has developed security against hacking methods potentially [15]. Moreover, a key image is generated based on a seed key exchanged in between both the sender and the receiver. The Euclidean distribution is optimally based on the worst clustering between the cover and key images. Finally, both least signification bit (LSB) and most signification bit (MSB) are used to physically hide the secret bits.

In this paper, an evaluation strategy for testing the effectiveness of the proposed system is presented. Technically, peak signal to noise ratio (PSNR), structural similarity index metric (SSIM), and reduced mean square error (MSE) have been used as quality metrics for evaluation and efficiency research. Twenty-five MRI images and three MRI image sizes were used to evaluate the achievement of the proposed system. The proposed model produced excellent results, especially when compared to other methods. The remainder of this work is structured as follows: section 2 includes related works. Section 3 includes proposed method. Section 4 is dedicated for experiments and results. In the end, conclusion is presented in section 5.

## 2. RELATED WORK

Shen *et al.* [16] emphasised high volume of networking technologies have been achieved with the target of telemedicine security. At the same time, great research has been produced by scholars resulted in large number of publications. Shivani [17] have addressed the problem of COVID-19 pandemic represented by the social distancing among patients that raised a significant reason to use healthcare electronic and telemedicine. This paper has proposed a watermarking for detecting the forged region at the other side for electronic healthcare applications. In order to support the proposed model achievement, PSNR, MSE, and SSIM have been calculated. The datasets have different image sizes of computed tomography and magnetic resonance imaging (CT-MRI) repository used for analysis and evaluation. The best results are: PSNR about 59, MSE about 0.06162 and SSIM about 0.99518. The proposed model has produced considerable results. However, there was little comparison between the suggested approach and other models in terms of PSNR and MSE. Furthermore, the findings of other models have outperformed the proposed model.

Devi *et al.* [18] have discussed the problem of the medical traveling information through the internet with medical internet of things (IoMT). This paper has presented steganography information in MRI brain image of the patient. Then, calculate accuracy for MRI brain image. The identity of the patient is hidden in the image MRI brain image using a spatial steganography method on T2-weighted MR images. The proposed model has been evaluated based on PSNR, SSIM, and BER. Various MR image datasets have been collected such as (dataset-75, dataset-160) from Harvard whole brain atlas [19]. PSNR about 37.72, MSE about 9.8575, and BER about 0.6808 have been achieved as best results. Despite the fact that the proposed system has produced considerable results, a large number of assessment samples were missing.

Mansour and Parah [11] has discussed the fact that cloud computing and IoT have better method for healthcare services but privacy and security of patient information have challenge in telemedicine. This article has proposed a new method of reversible data hiding approach based on lagrange's interpolation polynomial, secret sharing, and bit substitution for EHI security. The proposed model evaluation is based on PSNR metric. Many images have been used for evaluation analysis and best PSNR was about 52.

Cai *et al.* [20] have addressed the problem of the large amount of images construct of two parts region of interest (ROI) and background (BG). They have attempted to reduce the size of ROI without affecting its container of key information. This article has proposed a novel unified framework based on deep learning in order to obtain the optimization of rate distortion for ROI compression. The framework has included a pair of convolutional neural network (CNN) for encoder and decoder for ROI and a learned entropy codec. At the same time, CNN encoder has generated multi-scale representations for having efficient rate allocation and tacit mask of ROI to guide rate allocation. In order to validate the proposed system performance, PSNR, and processing time have been used. Additionally, the results of the proposed model have been compared with other models called JP2K, high efficiency video coding (HEVC). Practically, the proposed model has achieved PSNR about (22-37) while other models have obtained about (22-36) for both JP2K and HEVC. On the other hand, the processing time has reached about 530 for the proposed system whereas other models have obtained about 116 for JP2K. Four datasets: MSRA-B, ECSSD, LFW, and FDDB have been used for evaluation and testing purposes. PSNR about 37 and processing time about 530 have been obtained as best result. Although the proposed model have obtained high values, other models especially JP2K have achieved better results. Moreover, the performance metrics are insufficient because of their lacking for computing CR scale.

Gull *et al.* [21] have discussed the development in network technology in internet of medical and the challenge to save information of medical from hackers. The research paper has proposed a IoMT-based networks benefit from a reversible data concealing approach by using the huffman encoding. The method is efficient enough to conceal data in dual images while remaining undetectable. The proposed model has been evaluated based on PSNR, SSIM, various MR image datasets from waterloo gray scale images database and OPENi medical image (open access biomedical image search engine) dataset. Average percentage for PSNR is about 37.72 and SSIM is about 0.8873 representing the best results.

## 3. PROPOSED MODELS

This section present the proposed model. Moreover, it describes the techniques used for the embedding and extracting the secret information. First, Euclidean measurements are explained. Secondly, the proposed data distribution based on Euclidean is illustrated. Then, secret key generation model is stated and finally both least significant bit and most significant bit hiding models are explained.

### 3.1. Euclidean measurements

The Euclidean distance means the length of a straight line connecting two points [22], [23]. The minimum length distance measurement between two points is a major problem in many applications. In this paper, Euclidean distance is suggested to find the worst similitude as a method to ensure random positions selection for the hidden bits. In order to resolve this problem, the maximum distance is calculated between the cover image corresponding block of pixels and a randomly generated image key block [24]. Technically, each block have eight pixels. The main objective of this calculation is the determine the block indexes from the image key (i, j). Euclidean distance formula is defined by (1):

$$D = \sqrt[2]{\{(X2 - X1) + (Y2 - Y1)\}} \quad (1)$$

where D is the Euclidean distance; (x1, y1) is the coordination of the first point; and (x2, y2) is the coordination of the second point.

### 3.2. Euclidean distribution

With the aim to protect patient privacy from illegal access, a random secure distribution of secret text based on Euclidean similarity has been developed. Image is divided into RGB bands and based on that the red band is used as a Euclidean map for searching the secret positions and the blue band for hiding secret text. The red band is checked for the secret positions in comparison with blocks in the key image (i,j). The key image matrix is generated prior to the random distribution based on a random generation model. The destination block is the result of this process. Finally, indexes are extracted and utilised to conceal the secret text in the blue band. Figure 1 depicts the use of Euclidean similarity to conceal hidden content within a cover picture. Figure 2 depicts the extraction of hidden text that represent the patient private information.

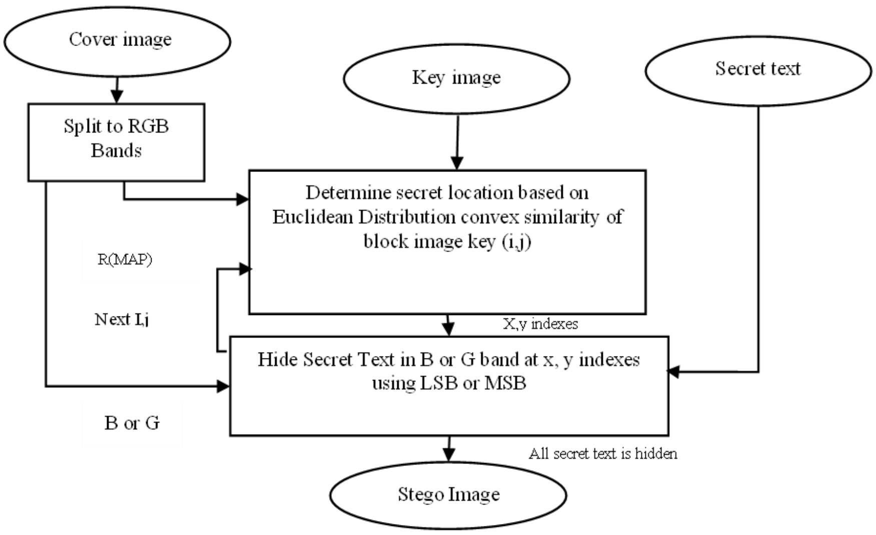


Figure 1. Proposed operating system for hiding

### 3.3. Key image generation

The key image is generated with the same size of the original cover image. Euclidean distance is calculated for the cover image block inside the key image in order to randomly find secret location. The key image is constructed on both sides for sender and receiver in an unexpected manner. Both secret seeds (seed1 and seed2) are defined on the sender side and receiver sides by using asymmetric method encryption. At the same moment, both the sender and the receiver have seed1 and seed2. Figure 3 shows the key image process for both the sender and the receiver.

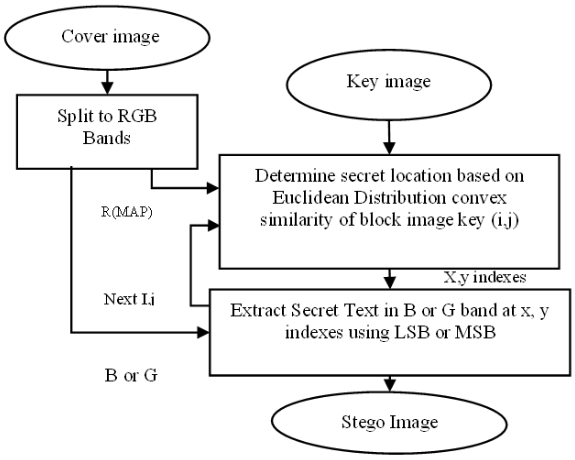


Figure 2. Proposed operating system for extraction

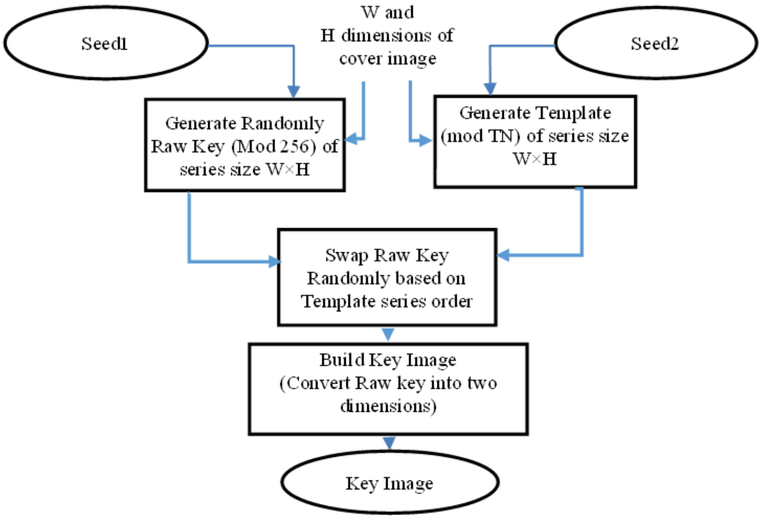


Figure 3. The key image process for both the sender and receiver

### 3.4. Least significant bit steganography technique LSB

It is the first developed hiding method for the proposed model. LSB embeds the information bits into the cover image by least significant bit in a sequence order. Actually the change is small because of the capacity, tamper the least-significant bit does not make a discernible difference. The hackers will check secret bits from the cover least successively. This is a common flaw in steganography approaches. To get secret bits, binary masking is used to extract the least significant bits from cover bands.

### 3.5. Most significant bit steganography technique MSB

MSB is considered as a very strong security technique with low computing complexity and minimal distortion of the gathering signal. This technique puts embedding patient information into specific places called special range numbers of the MRI images. This approach must be used to hide a secret bit in a high significant bit, with the resulting distortion being equivalent to LSB. The same technique is utilised for both hiding and extract secret information [25].
The MRI host is then shifted by (2):

$$S = Rmin + (M \bmod n) \tag{2}$$

where S is the resulting shifted value; Rmin is start value of the target special range; and n is length of the special range. We utilised Rmin=127, Rmax=129, and n=3 in our studies.

According (3), the set S of shifted values will be utilised as a gathering to disguise the secret bit B:

$$M_n = \begin{cases} M_o + (R_{max} - S) \; if \; B = 1 \\ M_o - (S - R_{min}) \; if \; B = 0 \end{cases} \quad (3)$$

where Mn is new resultant value of the host data; Rmin is minimum value of the selected special range; Rmax is maximum value of the selected special range; Mo is original host signal sample; and B is secret bit.

### 3.6. Embedding model

Technology of steganography has used LSB with Euclidean security distribution and MSB with Euclidean security distribution. First, seed1 and seed2 are predefined values to the embedding system. Then, the proposed model split RGB bands into R map that used to determine secret locations based on Euclidean distribution convex similarity of block image key (i,j) and B or G to hide secret text in B or G band at x, y indexes using LSB or MSB. Finally, (2) would be used to shift the cover byte first, and (3) would be used to hide the secret bit.

### 3.7. Information extraction

To extract hidden bits from the cover image, the recipient must first have the values for seed1 and seed2. The key image is then created using the same approach as on the transmitter and receiver sides. Extract hidden text by reverse the hiding technique by determining secret locations based on Euclidean distribution convex similarity of block image key (i,j). Finally, extract secret text from B or G bands at x, y indexes using LSB or MSB.

## 4. EXPERIMENTS AND RESULTS

With the aim to have an accurate evaluation, a dataset has been acquired by communicating the writer Abed [26] and used. Technically, the suggested model is tested and evaluated on many different sample images of MRI for by LSB Euclidean model and MSB Euclidean model.

### 4.1. Evaluation metrics

In this article, we use several evaluation metrics to evaluate the efficiency of our proposed system. The quality metric was determined by calculating PSNR, SSIM, and MSE. The evaluation results include comparisons between the new suggest model and other techniques of the MRI images after hiding information:

- PSNR: it calculates the stego image's imperceptibility [27]. A higher PSNR value indicates a higher quality of the stego image or a higher imperceptibility of the hidden message. It is also known as the peak square value of the pixels divided by MSE. It’s calculated by (4).

$$\text{PSNR} = 10.\log_{10}\left(\frac{Max^2}{MSE}\right) \quad (4)$$

- MSE: it calculates the volume of the average error between the embedded and the original MRI image. The error decreases as the MSE value decreases [28]. According to (5):

$$MSE = \frac{1}{MN}\sum_{i=1}^{M}\sum_{j=1}^{N}[I(i,j) - I`(i,j)] \quad (5)$$

where M, N the number of values MRI image sample (rows and columns of MRI image sample); I is the original MRI image sample; I` is the MRI image sample after steganography; and (I−I`) are Its different between MRI image sample before and after the steganography.

### 4.2. Analysis and comparisons

According to the data results provided in Tables 1-6, the suggested model has performed well when compared to the Abed [26] and Bander [29] methods. These results have demonstrated comparisons with PSNR, MSE, and SSIM measurements for the proposed model using the Abed [26] and Bander [29]. This evaluation was performed on both the LSB with Euclidean distribution and the MSB with Euclidean distribution. Sample images of MRI for three dimensions 125×125, 250×250, and 512×512 are tested respectively by the proposed model and the two other models.

Figure 4 displays the image original samples used in the experiments. Actually, the suggested model has outperformed the previous models with PSNR average of 71.476,061 and MSE average of

0.009,760,533. The obtained proposed results in Tables 1-3 are presented in band chart explained in Figures 5 and 6 represent the comparisons PSNR and MSE average for the proposed model with Abed and Bander methods for least significant bit Euclidean distribution. Moreover, the obtained proposed results in Tables 4-6 are presented in band chart explained in Figures 7 and 8 show comparisons of average PSNR and MSE for the proposed model with Abed and Bander methods for most significant bit Euclidean distribution.

Table 1. Comparative performance for proposed method LSB Euclidean, Abed and Bander methods of steganography images when images have 125×125 dimension

| Samples | Abed method | | Bander method | | The proposed method LSB Euclidean | | |
|---|---|---|---|---|---|---|---|
| file name | MSE | PSNR | MSE | PSNR | MSE | PSNR | SSIM |
| MRI1 | 1.809,728 | 45.554,67 | 0.049,603,7 | 61.175,66 | 0.0100,835,6 | 68.094,67 | 0.000,507,417 |
| MRI2 | 1.717,12 | 45.782,8 | 0.0492,624,7 | 61.205,64 | 0.0104,960,1 | 67.920,56 | 0.000,515,586 |
| MRI3 | 1.750,4 | 45.699,43 | 0.0455,443,7 | 61.546,46 | 0.0100,622,4 | 68.103,86 | 0.000,616,103 |
| MRI4 | 1.773,376 | 45.642,8 | 0.0531,511,9 | 60.875,67 | 0.009,969,784 | 68.143,94 | 0.000,578,804 |
| MRI5 | 1.812,928 | 45.547 | 0.0521,346,1 | 60.959,54 | 0.010,026,72 | 68.119,22 | 0.000,519,808 |
| MRI6 | 1.534,4 | 46.271,42 | 0.053,023,35 | 60.886,13 | 0.010,254,31 | 68.021,74 | 0.000,521,497 |
| MRI7 | 1.712,512 | 45.794,47 | 0.052,148,86 | 60.958,35 | 0.010,240,09 | 68.027,76 | 0.000,482,045 |
| MRI8 | 1.817,792 | 45.535,36 | 0.049,724,68 | 61.165,08 | 0.010,296,98 | 68.003,71 | 0.000,478,692 |
| MRI9 | 1.739,776 | 45.725,87 | 0.049,035,02 | 61.225,74 | 0.010,318,31 | 67.994,71 | 0.000,464,708 |
| MRI10 | 1.762,048 | 45.670,63 | 0.049,717,51 | 61.165,71 | 0.010,346,76 | 67.982,76 | 0.000,476,985 |
| MRI11 | 1.718,72 | 45.778,75 | - | - | 0.010,218,73 | 68.036,83 | 0.000,450,905 |
| MRI12 | 1.734,976 | 45.737,87 | - | - | 0.010,517,38 | 67.911,73 | 0.000,433,834 |
| MRI13 | 1.746,24 | 45.709,76 | - | - | 0.010,168,93 | 68.058,05 | 0.000,435,151 |
| MRI14 | 1.723,712 | 45.766,16 | - | - | 0.010,254,28 | 68.021,75 | 0.000,449,821 |
| MRI15 | 1.777,472 | 45.632,78 | - | - | 0.010,161,85 | 68.061,07 | 0.000,451,875 |
| MRI16 | 1.803,136 | 45.570,52 | - | - | 0.010,147,63 | 68.067,15 | 0.000,470,873 |
| MRI17 | 1.786,496 | 45.610,78 | - | - | 0.010,140,53 | 68.070,2 | 0.000,483,849 |
| MRI18 | 1.695,04 | 45.839 | - | - | 0.010,069,42 | 68.100,76 | 0.000,486,936 |
| MRI19 | 1.805,568 | 45.564,67 | - | - | 0.010,332,54 | 67.988,73 | 0.000,471,975 |
| MRI20 | 1.787,392 | 45.608,61 | - | - | 0.010,190,31 | 68.048,93 | 0.000,445,069 |
| MRI21 | 1.722,432 | 45.769,38 | - | - | 0.010,062,24 | 68.103,86 | 0.000,813,24 |
| MRI22 | 1.754,24 | 45.689,91 | - | - | 0.009,934,224 | 68.159,46 | 0.000,908,914 |
| MRI23 | 1.724,928 | 45.763,09 | - | - | 0.010,154,66 | 68.064,15 | 0.000,895,459 |
| MRI24 | 1.735,168 | 45.737,39 | - | - | 0.010,048,01 | 68.110,01 | 0.000,913,954 |
| MRI25 | 1.733,696 | 45.741,07 | - | - | 0.009,969,779 | 68.143,95 | 0.000,924,114 |
| Avg | 1.747,171,84 | 45.709,767,6 | 0.050,335 | 61.116,4 | 0.0101,786,11 | 68.054,382,4 | 0.000,567,905 |

Table 2. Comparative performance for proposed method LSB Euclidean, Abed and Bander methods of steganography images when images have 250×250 dimension

| Samples | Abed method | | Bander method | | The proposed method LSB Euclidean | | |
|---|---|---|---|---|---|---|---|
| file name | MSE | PSNR | MSE | PSNR | MSE | PSNR | SSIM |
| MRI1 | 1.977,36 | 45.169,946,16 | 0.046,625,5 | 61.444,57 | 0.002,472,883 | 74.198,77 | 0.000,483,094 |
| MRI2 | 1.887,008 | 45.373,066,2 | 0.046,650,39 | 61.442,25 | 0.002,479,995 | 74.186,29 | 0.000,489,908 |
| MRI3 | 1.926,112 | 45.283,988,24 | 0.045,674,61 | 61.534,05 | 0.002,590,232 | 73.997,41 | 0.000,586,842 |
| MRI4 | 1.896,288 | 45.351,760,64 | 0.053,457,55 | 60.850,71 | 0.002,527,999 | 74.103,03 | 0.000,553,205 |
| MRI5 | 2.029,44 | 45.057,041,45 | 0.053,198,07 | 60.871,85 | 0.002,424,906 | 74.283,85 | 0.000,496,897 |
| MRI6 | 1.699,856 | 45.826,682,28 | 0.053,635,32 | 60.836,3 | 0.002,494,248 | 74.161,41 | 0.000,499,059 |
| MRI7 | 1.870,224 | 45.411,867,35 | 0.053,757,94 | 60.826,38 | 0.002,517,352 | 74.121,36 | 0.000,458,568 |
| MRI8 | 1.948,48 | 45.233,844,08 | 0.046,367,79 | 61.468,64 | 0.002,654,237 | 73.891,4 | 0.000,455,314 |
| MRI9 | 1.918,208 | 45.301,846,63 | 0.046,174,05 | 61.486,82 | 0.002,597,351 | 73.985,5 | 0.000,442,447 |
| MRI10 | 1.942,992 | 45.246,093,48 | 0.046,431,77 | 61.462,65 | 0.002,567,129 | 74.036,32 | 0.000,453,84 |
| MRI11 | 1.845,664 | 45.469,277,2 | - | - | 0.002,544,011 | 74.075,61 | 0.000,429,466 |
| MRI12 | 1.932,288 | 45.270,085,04 | - | - | 0.002,533,34 | 74.093,87 | 0.000,414,45 |
| MRI13 | 1.903,264 | 45.335,813,28 | - | - | 0.002,563,56 | 74.042,37 | 0.000,415,28 |
| MRI14 | 1.914,032 | 45.311,311,67 | - | - | 0.002,526,232 | 74.106,07 | 0.000,429,325 |
| MRI15 | 1.964,704 | 45.197,832,32 | - | - | 0.002,577,787 | 74.018,33 | 0.000,430,797 |
| MRI16 | 1.967,52 | 45.191,612,05 | - | - | 0.002,552,904 | 74.060,46 | 0.000,448,807 |
| MRI17 | 1.974,48 | 45.176,276,22 | - | - | 0.002,563,568 | 74.042,36 | 0.000,461,448 |
| MRI18 | 1.868,048 | 45.416,923,3 | - | - | 0.002,622,236 | 73.944,08 | 0.000,464,164 |
| MRI19 | 1.958,48 | 45.211,612,2 | - | - | 0.002,544,012 | 74.075,61 | 0.000,451,364 |
| MRI20 | 1.957,088 | 45.214,700,07 | - | - | 0.002,538,682 | 74.084,72 | 0.000,426,846 |
| MRI21 | 1.912,4 | 45.315,016,26 | - | - | 0.002,556,452 | 74.054,43 | 0.000,741,26 |
| MRI22 | 1.907,536 | 45.326,076,18 | - | - | 0.002,535,114 | 74.090,83 | 0.000,812,215 |
| MRI23 | 1.904,24 | 45.333,586,77 | - | - | 0.002,522,665 | 74.112,21 | 0.000,797,848 |
| MRI24 | 1.903,584 | 45.335,083,15 | - | - | 0.002,538,665 | 74.084,75 | 0.000,808,855 |
| MRI25 | 1.915,632 | 45.307,682,78 | - | - | 0.002,561,776 | 74.045,39 | 0.000,819,037 |
| Avg | 1.916,997,12 | 45.306,761 | 0.049,197 | 61.222,42 | 0.002,544,293 | 74.075,857,2 | 0.000,530,813 |

Table 3. Comparative performance for proposed method LSB Euclidean, Abed and Bander methods of steganography images when images have 512×512 dimension

| Samples | Abed method | | Bander method | | The proposed method LSB Euclidean | | |
|---|---|---|---|---|---|---|---|
| File name | MSE | PSNR | MSE | PSNR | MSE | PSNR | SSIM |
| MRI1 | 2.036,514,282 | 45.041,929,01 | 0.173,030,2 | 55.749,58 | 0.000,601,874 | 80.335,75 | 0.000,444,783 |
| MRI2 | 1.877,239,227 | 45.395,607,4 | 0.168,251,9 | 55.871,2 | 0.000,616,285 | 80.232,99 | 0.000,449,758 |
| MRI3 | 1.924,274,445 | 45.288,133,49 | 0.152,725,9 | 56.291,68 | 0.000,612,472 | 80.259,94 | 0.000,532,301 |
| MRI4 | 1.911,251,068 | 45.317,626,2 | 0.180,751,3 | 55.559,99 | 0.000,628,577 | 80.147,22 | 0.000,504,928 |
| MRI5 | 1.943,630,219 | 45.244,667,18 | 0.186,858,7 | 55.415,67 | 0.000,607,812 | 80.293,11 | 0.000,454,584 |
| MRI6 | 1.737,731,934 | 45.730,975,79 | 0.179,157,9 | 55.598,45 | 0.000,602,73 | 80.329,57 | 0.000,457,285 |
| MRI7 | 1.914,749,146 | 45.309,684,76 | 0.177,800,1 | 55.631,48 | 0.000,618,835 | 80.215,06 | 0.000,426,649 |
| MRI8 | 1.941,310,883 | 45.249,852,72 | 0.172,973,2 | 55.751,01 | 0.000,603,576 | 80.323,49 | 0.000,424,238 |
| MRI9 | 1.932,186,127 | 45.270,314,01 | 0.170,050,7 | 55.825,02 | 0.000,603,151 | 80.326,55 | 0.000,412,074 |
| MRI10 | 1.937,366,486 | 45.258,685,78 | 0.167,953,4 | 55.878,92 | 0.000,618,835 | 80.215,06 | 0.000,422,717 |
| MRI11 | 1.913,192,749 | 45.313,216,35 | - | - | 0.000,597,64 | 80.366,41 | 0.000,401,056 |
| MRI12 | 1.936,374,664 | 45.260,909,69 | - | - | 0.000,598,91 | 80.357,19 | 0.000,387,797 |
| MRI13 | 1.896,503,448 | 45.351,267,24 | - | - | 0.000,596,791 | 80.372,58 | 0.000,388,028 |
| MRI14 | 1.939,590,454 | 45.253,703,23 | - | - | 0.000,604,42 | 80.317,41 | 0.000,399,91 |
| MRI15 | 1.939,495,087 | 45.253,916,77 | - | - | 0.000,615,441 | 80.238,94 | 0.000,401,995 |
| MRI16 | 1.905,849,457 | 45.329,917,68 | - | - | 0.000,624,343 | 80.176,57 | 0.000,417,068 |
| MRI17 | 1.909,034,729 | 45.322,665,32 | - | - | 0.000,625,615 | 80.167,73 | 0.000,429,007 |
| MRI18 | 1.902,450,562 | 45.337,669,81 | - | - | 0.000,614,596 | 80.244,9 | 0.000,432,308 |
| MRI19 | 1.916,313,171 | 45.306,138,76 | - | - | 0.000,604,847 | 80.314,35 | 0.000,420,778 |
| MRI20 | 1.945,339,203 | 45.240,850,22 | - | - | 0.000,613,324 | 80.253,91 | 0.000,399,277 |
| MRI21 | 1.928,749,084 | 45.278,046,28 | - | - | 0.000,613,318 | 80.253,94 | 0.000,655,787 |
| MRI22 | 1.894,256,592 | 45.356,415,54 | - | - | 0.000,605,265 | 80.311,35 | 0.000,708,241 |
| MRI23 | 1.894,332,886 | 45.356,240,62 | - | - | 0.000,601,45 | 80.338,81 | 0.000,697,408 |
| MRI24 | 1.894,226,074 | 45.356,485,5 | - | - | 0.000,608,655 | 80.287,09 | 0.000,710,42 |
| MRI25 | 1.894,226,074 | 45.356,485,5 | - | - | 0.000,606,96 | 80.299,21 | 0.000,718,02 |
| Avg | 1.914,647,522 | 45.311,256,19 | 0.1729,55 | 55.757,3 | 0.000,609,829 | 80.279,165,2 | 0.000,483,857 |

Table 4. Comparative performance for proposed method MSB Euclidean, Abed and Bander methods of steganography images when images have 125×125 dimension

| Samples | Abed method | | Bander method | | The proposed method MSB Euclidean | | |
|---|---|---|---|---|---|---|---|
| file name | MSE | PSNR | MSE | PSNR | MSE | PSNR | SSIM |
| MRI1 | 1.218,56 | 47.272,334,43 | 0.044,782,58 | 61.619,71 | 0.034,894,59 | 62.703,22 | 0.000,507,523 |
| MRI2 | 1.205,76 | 47.318,194,88 | 0.044,671,73 | 61.630,47 | 0.034,147,88 | 62.797,16 | 0.000,515,649 |
| MRI3 | 1.213,568 | 47.290,162,45 | 0.044,052,97 | 61.691,05 | 0.035,427,95 | 62.637,34 | 0.000,616,155 |
| MRI4 | 1.220,288 | 47.266,180,2 | 0.054,816,56 | 60.741,69 | 0.035,243,11 | 62.660,06 | 0.000,578,84 |
| MRI5 | 1.150,4 | 47.522,314,88 | 0.054,595,3 | 60.759,25 | 0.033,259,14 | 62.911,69 | 0.000,519,872 |
| MRI6 | 1.137,28 | 47.572,129,59 | 0.054,021,13 | 60.805,17 | 0.032,469,85 | 63.016 | 0.000,521,578 |
| MRI7 | 1.241,6 | 47.190,986,57 | 0.054,855,63 | 60.738,59 | 0.035,256,9 | 62.658,36 | 0.000,482,069 |
| MRI8 | 1.249,024 | 47.165,095,77 | 0.044,049,15 | 61.691,43 | 0.035,847,16 | 62.586,25 | 0.000,478,746 |
| MRI9 | 1.241,344 | 47.191,882,11 | 0.044,102,66 | 61.686,16 | 0.034,993,95 | 62.690,87 | 0.000,464,734 |
| MRI10 | 1.239,232 | 47.199,277,41 | 0.044,182,93 | 61.678,26 | 0.0349,15,67 | 62.700,6 | 0.000,476,981 |
| MRI11 | 1.244,416 | 47.181,147,74 | - | - | 0.0346,383,6 | 62.735,23 | 0.000,450,895 |
| MRI12 | 1.231,424 | 47.226,727,47 | - | - | 0.0337,282,2 | 62.850,87 | 0.000,433,873 |
| MRI13 | 1.257,6 | 47.135,378,32 | - | - | 0.0351,717,4 | 62.668,87 | 0.000,435,131 |
| MRI14 | 1.238,848 | 47.200,623,37 | - | - | 0.033,379,76 | 62.895,97 | 0.000,449,81 |
| MRI15 | 1.233,024 | 47.221,088,31 | - | - | 0.035,726,35 | 62.600,92 | 0.000,451,889 |
| MRI16 | 1.268,544 | 47.097,748,25 | - | - | 0.034,225,97 | 62.787,25 | 0.000,470,905 |
| MRI17 | 1.257,6 | 47.135,378,32 | - | - | 0.035,335,31 | 62.648,72 | 0.000,483,913 |
| MRI18 | 1.199,424 | 47.341,076,26 | - | - | 0.035,285,43 | 62.654,85 | 0.000,487 |
| MRI19 | 1.265,088 | 47.109,596,25 | - | - | 0.035,690,77 | 62.605,24 | 0.000,471,997 |
| MRI20 | 1.265,088 | 47.109,596,25 | - | - | 0.033,891,71 | 62.829,87 | 0.000,445,075 |
| MRI21 | 1.213,184 | 47.291,536,87 | - | - | 0.034,417,95 | 62.762,95 | 0.000,813,232 |
| MRI22 | 1.230,08 | 47.231,470,04 | - | - | 0.033,713,99 | 62.852,7 | 0.000,908,888 |
| MRI23 | 1.215,872 | 47.281,925,04 | - | - | 0.033,699,77 | 62.854,53 | 0.000,895,468 |
| MRI24 | 1.225,216 | 47.248,677,01 | - | - | 0.034,439,28 | 62.760,26 | 0.000,913,964 |
| MRI25 | 1.228,352 | 47.237,575,24 | - | - | 0.033,223,37 | 62.916,37 | 0.000,924,144 |
| Avg | 1.227,632,64 | 47.241,524,12 | 0.048,413 | 61.304,18 | 0.034,520,967 | 62.751,446 | 0.000,567,933 |

Table 5. Comparative performance for proposed method MSB Euclidean, Abed and Bander methods of steganography images when images have 250×250 dimension

| Samples | Abed method | | Bander method | | The proposed method MSB Euclidean | | |
|---|---|---|---|---|---|---|---|
| file name | MSE | PSNR | MSE | PSNR | MSE | PSNR | SSIM |
| MRI1 | 1.326,784 | 46.902,8 | 0.163,280,9 | 56.001,45 | 0.008,520,981 | 68.825,9 | 0.000,483,128 |
| MRI2 | 1.315,04 | 46.941,41 | 0.159,564,7 | 56.101,43 | 0.008,744,99 | 68.713,21 | 0.000,489,927 |
| MRI3 | 1.320,816 | 46.922,38 | 0.153,203,5 | 56.278,11 | 0.008,961,883 | 68.606,81 | 0.000,586,856 |
| MRI4 | 1.320,208 | 46.924,38 | 0.185,911,7 | 55.437,74 | 0.008,531,664 | 68.820,47 | 0.000,553,228 |
| MRI5 | 1.246,896 | 47.172,5 | 0.184,281,8 | 55.475,98 | 0.008,124,56 | 69.032,81 | 0.000,496,909 |
| MRI6 | 1.247,68 | 47.169,77 | 0.178,968,2 | 55.603,05 | 0.007,872,115 | 69.169,89 | 0.000,499,077 |
| MRI7 | 1.379,92 | 46.732,26 | 0.179,160,8 | 55.598,37 | 0.008,689,787 | 68.740,72 | 0.000,458,572 |
| MRI8 | 1.357,824 | 46.802,37 | 0.163,484,8 | 55.996,03 | 0.008,334,262 | 68.922,13 | 0.000,455,311 |
| MRI9 | 1.373,456 | 46.752,66 | 0.159,075,6 | 56.114,77 | 0.008,592,041 | 68.789,84 | 0.000,442,489 |
| MRI10 | 1.370,688 | 46.761,42 | 0.160,390,7 | 56.079,01 | 0.008,887,142 | 68.643,18 | 0.000,453,843 |
| MRI11 | 1.355,392 | 46.810,15 | - | - | 0.008,615,161 | 68.778,17 | 0.000,429,466 |
| MRI12 | 1.366,736 | 46.773,96 | - | - | 0.008,496,066 | 68.838,62 | 0.000,414,457 |
| MRI13 | 1.368,528 | 46.768,27 | - | - | 0.008,721,835 | 68.724,72 | 0.000,415,304 |
| MRI14 | 1.351,408 | 46.822,94 | - | - | 0.008,588,494 | 68.791,63 | 0.000,429,323 |
| MRI15 | 1.384,176 | 46.718,89 | - | - | 0.008,896,044 | 68.638,83 | 0.000,430,801 |
| MRI16 | 1.380,256 | 46.731,21 | - | - | 0.009,068,483 | 68.555,46 | 0.000,448,816 |
| MRI17 | 1.379,664 | 46.733,07 | - | - | 0.008,565,372 | 68.803,34 | 0.000,461,452 |
| MRI18 | 1.369,408 | 46.765,48 | - | - | 0.008,634,685 | 68.768,34 | 0.000,464,179 |
| MRI19 | 1.398,96 | 46.672,75 | - | - | 0.008,645,353 | 68.762,98 | 0.000,451,375 |
| MRI20 | 1.414,512 | 46.624,74 | - | - | 0.008,917,352 | 68.628,44 | 0.000,426,841 |
| MRI21 | 1.338,048 | 46.866,09 | - | - | 0.008,833,836 | 68.669,31 | 0.000,741,249 |
| MRI22 | 1.331,008 | 46.889 | - | - | 0.008,245,392 | 68.968,69 | 0.000,812,208 |
| MRI23 | 1.337,536 | 46.867,75 | - | - | 0.008,515,613 | 68.828,64 | 0.000,797,832 |
| MRI24 | 1.327,408 | 46.900,76 | - | - | 0.008,675,615 | 68.747,8 | 0.000,808,844 |
| MRI25 | 1.339,472 | 46.861,47 | - | - | 0.008,606,271 | 68.782,65 | 0.000,819,035 |
| Avg | 1.348,072,96 | 46.835,539,2 | 0.168,732 | 55.868,59 | 0.008,611,4 | 68.782,103,2 | 0.000,530,821 |

Table 6. Comparative performance for proposed method MSB Euclidean, Abed and Bander methods of steganography images when images have 512×512 dimension

| Samples | Abed method | | Bander method | | The proposed method MSB Euclidean | | |
|---|---|---|---|---|---|---|---|
| file name | MSE | PSNR | MSE | PSNR | MSE | PSNR | SSIM |
| MRI1 | 1.335,838,3 | 46.873,26 | 0.155,255,1 | 56.220,34 | 0.002,109,972 | 74.888,04 | 0.000,444,792 |
| MRI2 | 1.340,171,8 | 46.859,2 | 0.153,409,2 | 56.272,29 | 0.002,156,601 | 74.793,11 | 0.000,449,765 |
| MRI3 | 1.320,217,1 | 46.924,35 | 0.146,994,3 | 56.457,8 | 0.002,165,498 | 74.775,22 | 0.000,532,31 |
| MRI4 | 1.325,088,5 | 46.908,35 | 0.190,139,7 | 55.340,08 | 0.002,118,034 | 74.871,48 | 0.000,504,938 |
| MRI5 | 1.271,926,9 | 47.086,18 | 0.190,152,6 | 55.339,78 | 0.002,076,065 | 74.958,4 | 0.000,454,586 |
| MRI6 | 1.347,835,5 | 46.834,43 | 0.183,803 | 55.487,28 | 0.002,148,547 | 74.809,36 | 0.000,457,292 |
| MRI7 | 1.397,689,8 | 46.676,7 | 0.181,969 | 55.530,83 | 0.002,173,538 | 74.759,13 | 0.000,426,647 |
| MRI8 | 1.382,453,9 | 46.724,3 | 0.152,328,9 | 56.302,98 | 0.002,058,251 | 74.995,82 | 0.000,424,238 |
| MRI9 | 1.393,726,3 | 46.689,03 | 0.152,214,3 | 56.306,25 | 0.002,109,538 | 74.888,93 | 0.000,412,078 |
| MRI10 | 1.383,258,8 | 46.721,77 | 0.152,964,5 | 56.284,9 | 0.002,131,999 | 74.842,93 | 0.000,422,716 |
| MRI11 | 1.395,195 | 46.684,45 | - | - | 0.002,088,349 | 74.932,77 | 0.000,401,053 |
| MRI12 | 1.390,77 | 46.698,25 | - | - | 0.002,079,029 | 74.952,2 | 0.000,387,796 |
| MRI13 | 1.373,256,7 | 46.753,29 | - | - | 0.002,107,422 | 74.893,29 | 0.000,388,032 |
| MRI14 | 1.389,888,8 | 46.701 | - | - | 0.002,044,273 | 75.025,41 | 0.000,399,856 |
| MRI15 | 1.392,303,5 | 46.693,46 | - | - | 0.002,029,436 | 75.057,05 | 0.000,401,994 |
| MRI16 | 1.389,461,5 | 46.702,34 | - | - | 0.002,073,936 | 74.962,85 | 0.000,417,062 |
| MRI17 | 1.391,059,9 | 46.697,35 | - | - | 0.002,118,438 | 74.870,64 | 0.000,429,004 |
| MRI18 | 1.399,311,1 | 46.671,66 | - | - | 0.002,109,958 | 74.888,06 | 0.000,432,316 |
| MRI19 | 1.397,037,5 | 46.678,72 | - | - | 0.002,118,439 | 74.870,64 | 0.000,420,785 |
| MRI20 | 1.414,386,7 | 46.625,12 | - | - | 0.002,069,696 | 74.971,74 | 0.000,399,277 |
| MRI21 | 1.343,940,7 | 46.847 | - | - | 0.002,148,541 | 74.809,36 | 0.000,655,785 |
| MRI22 | 1.344,245,9 | 46.846,02 | - | - | 0.002,054,442 | 75.003,86 | 0.000,708,24 |
| MRI23 | 1.340,816,5 | 46.857,11 | - | - | 0.002,099,793 | 74.909,04 | 0.000,697,387 |
| MRI24 | 1.349,533,1 | 46.828,97 | - | - | 0.002,035,364 | 75.044,38 | 0.000,710,425 |
| MRI25 | 1.344,207,8 | 46.846,14 | - | - | 0.002,027,314 | 75.061,59 | 0.000,718,124 |
| Avg | 1.366,144,864 | 46.777,138 | 0.165,923 | 55.954,25 | 0.002,098,099 | 74.913,412 | 0.000,483,86 |

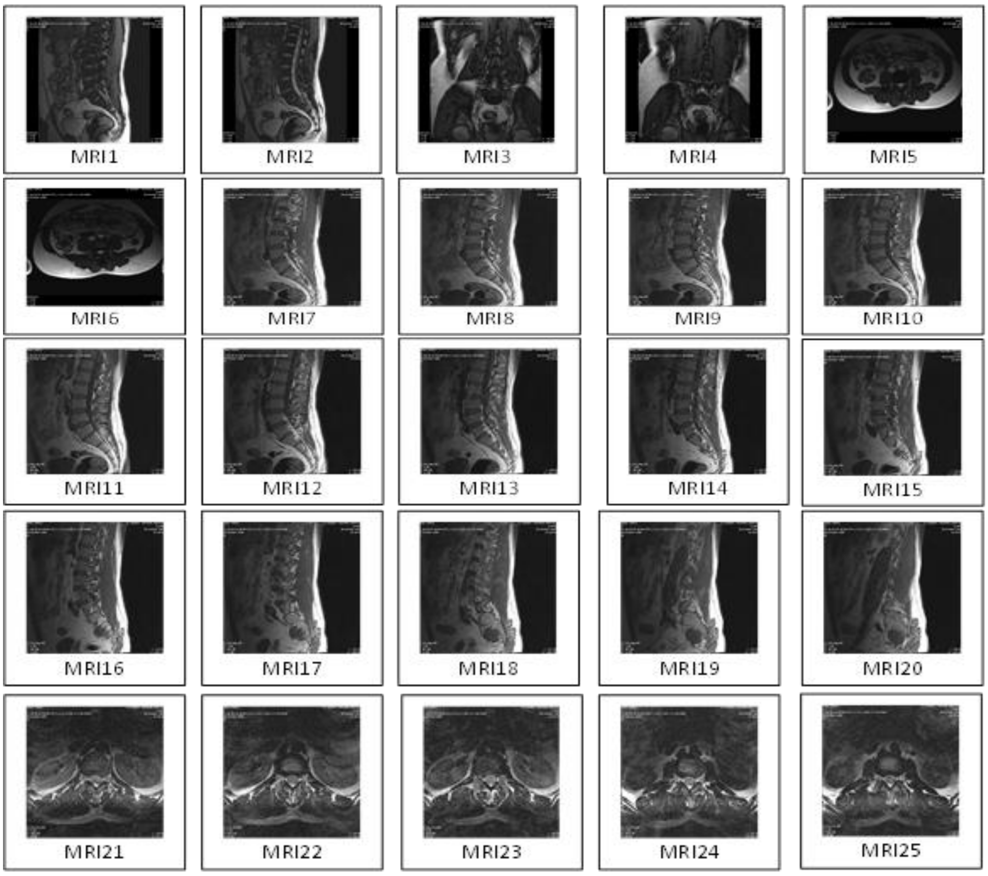


Figure 4. Original samples images MRI

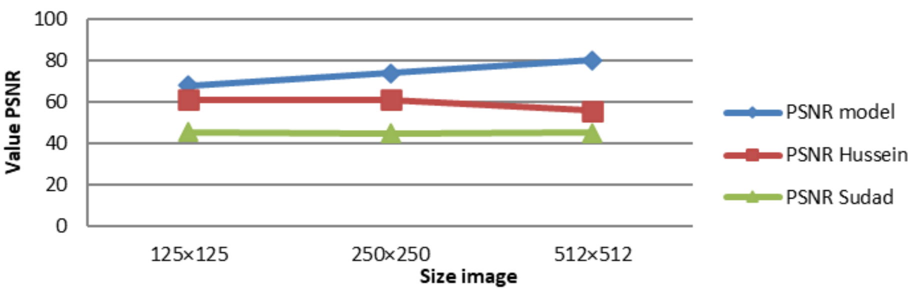


Figure 5. Average for PSNR results for proposed model, Abed [26] and Bander [29] for LSB Euclidean

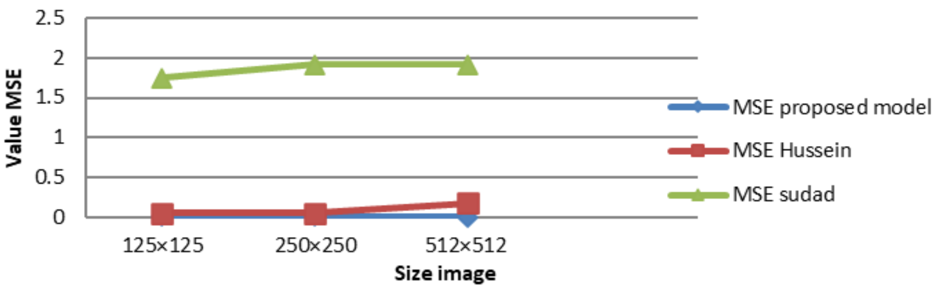


Figure 6. Average for MSE results for proposed model, Abed [26] and Bander [29] methods for LSB Euclidean

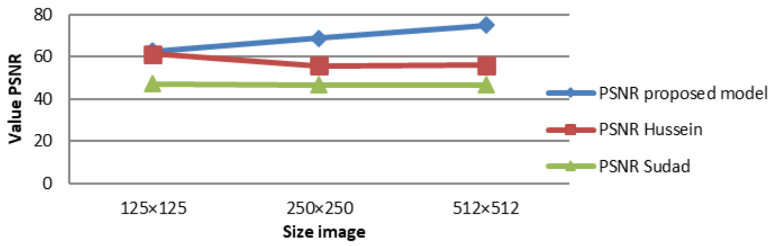


Figure 7. Average for PSNR results for proposed model, Abed [26] and Bander [29] for MSB Euclidean

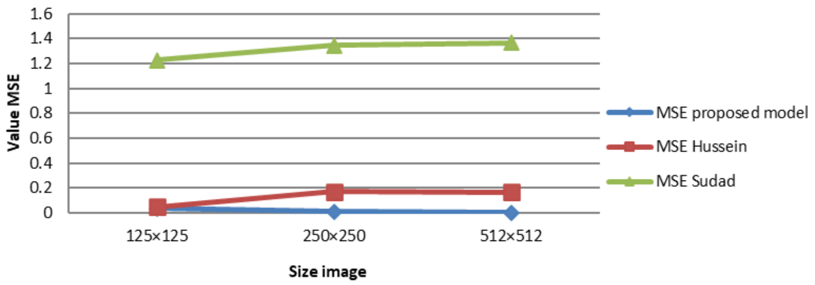


Figure 8. Average for MSE results for proposed model, Abed [26] and Bander [29] for MSB Euclidean

## 5. CONCLUSION

In conclusion, the new proposed model has provided more strong technique in patient secure information in cover image based on least significant bit Euclidean distribution or most significant bit Euclidean distribution. Furthermore, PSNR, MSE, and SSIM are calculated technically for the analysis and comparison process. Moreover, twenty-five MRI samples with dimensions of 125×125, 250×250, and 512×512 are chosen as the core dataset for evaluation. Finally, the new proposed model has shown better achievement and security in comparison with all other models.

## ACKNOWLEDGMENTS

We would like to express my sincere gratitude to Dr. Dhiah Al-Shammary for his invaluable scientific support and guidance throughout this research endeavor.

## REFERENCES

[1] A. J. T. Albderi, L. Ben Said, and D. Al-Shammary, “Literature Review for Health Secure Image Steganography and Visual Encryption,” in *2023 Al-Sadiq International Conference on Communication and Information Technology (AICCIT)*, 2023, pp. 218–223.

[2] A. T. Suhail and H. G. Ayoub, “A new method for hiding a secret file in several WAV files depends on circular secret key,” *Egyptian Informatics Journal*, vol. 23, no. 4, pp. 33–43, Dec. 2022, doi: 10.1016/j.eij.2022.06.003.

[3] J. J. Hathaliya and S. Tanwar, “An exhaustive survey on security and privacy issues in Healthcare 4.0,” *Computer Communications*, vol. 153, no. September 2019, pp. 311–335, 2020, doi: 10.1016/j.comcom.2020.02.018.

[4] L. K. Gupta, A. Singh, A. Kushwaha, and A. Vishwakarma, “Analysis of image steganography techniques for different image format,” *Proceedings of the 2021 1st International Conference on Advances in Electrical, Computing, Communications and Sustainable Technologies, ICAECT 2021*, 2021, doi: 10.1109/ICAECT49130.2021.9392492.

[5] D. R. I. M. Setiadi, “Improved payload capacity in LSB image steganography uses dilated hybrid edge detection,” *Journal of King Saud University - Computer and Information Sciences*, vol. 34, no. 2, pp. 104–114, 2022, doi: 10.1016/j.jksuci.2019.12.007.

[6] K. Chen and C. C. Chang, “High-capacity reversible data hiding in encrypted images based on extended run-length coding and block-based MSB plane rearrangement,” *Journal of Visual Communication and Image Representation*, vol. 58, pp. 334–344, 2019, doi: 10.1016/j.jvcir.2018.12.023.

[7] A. J. T. Albderi, L. Ben Said, and D. Al-Shammary, “Literature Review for Health Secure Image Steganography and Visual Encryption,” in *AICCIT 2023 - Al-Sadiq International Conference on Communication and Information Technology*, Jul. 2023, pp. 218–223, doi: 10.1109/AICCIT57614.2023.10217847.

[8] F. Al-Shaarani and A. Gutub, “Securing matrix counting-based secret-sharing involving crypto steganography,” *Journal of King Saud University - Computer and Information Sciences*, vol. 34, no. 9, pp. 6909–6924, 2022, doi: 10.1016/j.jksuci.2021.09.009.

[9] P. Panwar, S. Dhall, and S. Gupta, “A multilevel secure information communication model for healthcare systems,” *Multimedia Tools and Applications*, vol. 80, no. 5, pp. 8039–8062, 2021, doi: 10.1007/s11042-020-10083-5.

[10] M. Sookhak, M. R. Jabbarpour, N. S. Safa, and F. R. Yu, “Blockchain and smart contract for access control in healthcare: A survey, issues and challenges, and open issues,” *Journal of Network and Computer Applications*, vol. 178, no. December 2020, p.

102950, 2021, doi: 10.1016/j.jnca.2020.102950.
[11] R. F. Mansour and S. A. Parah, "Reversible Data Hiding for Electronic Patient Information Security for Telemedicine Applications," *Arabian Journal for Science and Engineering*, vol. 46, no. 9, pp. 9129–9144, 2021, doi: 10.1007/s13369-021-05716-2.
[12] D. Wu, F. E. Wolter, B. Wang, and L. Xie, "Searching for the shortest path to voltage instability boundary: From Euclidean space to algebraic manifold," *International Journal of Electrical Power and Energy Systems*, vol. 131, no. September 2020, p. 107127, 2021, doi: 10.1016/j.ijepes.2021.107127.
[13] H. Sajedi and S. R. Yaghobi, "Information hiding methods for E-Healthcare," *Smart Health*, vol. 15, no. December 2019, p. 100104, 2020, doi: 10.1016/j.smhl.2019.100104.
[14] Y. Wang and W. He, "High Capacity Reversible Data Hiding in Encrypted Image Based on Adaptive MSB Prediction," *IEEE Transactions on Multimedia*, vol. 24, no. c, pp. 1288–1298, 2022, doi: 10.1109/TMM.2021.3062699.
[15] A. Jaber, T. Albderi, D. Al-Shammary, and L. Ben, "Jaccard-based Random Distribution with Least and Most Significant Bit Hiding Methods for Highly Patients MRI Protected Privacy," vol. 7, no. November, pp. 1032–1040, 2023.
[16] Y. T. Shen, L. Chen, W. W. Yue, and H. X. Xu, "Digital Technology-Based Telemedicine for the COVID-19 Pandemic," *Frontiers in Medicine*, vol. 8, no. July, pp. 1–23, 2021, doi: 10.3389/fmed.2021.646506.
[17] S. Shivani, "Verifiable medical images for E-healthcare: A novel watermarking approach using robust bit-wise association of self-mutating offsprings of pixels," *Microprocessors and Microsystems*, vol. 90, no. February, p. 104483, 2022, doi: 10.1016/j.micpro.2022.104483.
[18] S. Devi, M. N. Sahoo, K. Muhammad, W. Ding, and S. Bakshi, "Hiding medical information in brain MR images without affecting accuracy of classifying pathological brain," *Future Generation Computer Systems*, vol. 99, pp. 235–246, 2019, doi: 10.1016/j.future.2019.01.047.
[19] M. Totten, "Letter from cuba," *World Affairs*, vol. 176, no. 6, pp. 31–37, 2014, doi: 10.1353/cal.2003.0015.
[20] C. Cai, L. Chen, X. Zhang, and Z. Gao, "End-to-End Optimized ROI Image Compression," *IEEE Transactions on Image Processing*, vol. 29, no. 8, pp. 3442–3457, 2020, doi: 10.1109/TIP.2019.2960869.
[21] S. Gull, S. A. Parah, and K. Muhammad, "Reversible data hiding exploiting Huffman encoding with dual images for IoMT based healthcare," *Computer Communications*, vol. 163, no. September, pp. 134–149, 2020, doi: 10.1016/j.comcom.2020.08.023.
[22] C. R. Giannella, "Instability results for Euclidean distance, nearest neighbor search on high dimensional Gaussian data," *Information Processing Letters*, vol. 169, p. 106115, 2021, doi: 10.1016/j.ipl.2021.106115.
[23] S. Marukatat and I. Methasate, "Fast nearest neighbor retrieval using randomized binary codes and approximate Euclidean distance," *Pattern Recognition Letters*, vol. 34, no. 9, pp. 1101–1107, 2013, doi: 10.1016/j.patrec.2013.03.006.
[24] M. Fampa, "Insight into the computation of Steiner minimal trees in Euclidean space of general dimension," *Discrete Applied Mathematics*, vol. 308, pp. 4–19, 2022, doi: 10.1016/j.dam.2019.03.015.
[25] A. Ibaida, I. Khalil, and D. Al-Shammary, "Embedding patients confidential data in ECG signal for healthcare information systems," *2010 Annual International Conference of the IEEE Engineering in Medicine and Biology Society, EMBC'10*, pp. 3891–3894, 2010, doi: 10.1109/IEMBS.2010.5627671.
[26] S. N. Abed, "Secure Distribution for LSB and MSB," 2019.
[27] A. Tanchenko, "Visual-PSNR measure of image quality," *Journal of Visual Communication and Image Representation*, vol. 25, no. 5, pp. 874–878, 2014, doi: 10.1016/j.jvcir.2014.01.008.
[28] F. Xue, Z. Ye, W. Lu, H. Liu, and B. Li, "MSE period based estimation of first quantization step in double compressed JPEG images," *Signal Processing: Image Communication*, vol. 57, no. March, pp. 76–83, 2017, doi: 10.1016/j.image.2017.05.008.
[29] H. K. Bander, "High Secure Distribution for Health Visual Patient Privacy," 2022.

## BIOGRAPHIES OF AUTHORS

**Ali Jaber Tayh Albderi** received the B.Sc. degree in Computer Science from AL Mustansiriya University, Baghdad, in 2004, the M.S degrees in Computer Network and Telecommunication from Voronezh High Technologies Institute, Russian Federation, in 2010. And now study Ph.D. degrees in computer science in University of Tunis (ISG-Campus), Tunis, Tunisia. His research interests include image, big data in network, cloud computer, network, security of multimedia, and encoding techniques. He can be contacted at email: ali.jaber.tayh@gmail.com.

**Lamjed Ben Said** received the B.Sc. degree in Computer Science with Management from the University of Tunis (ISG-Campus), Tunis, Tunisia, in 1998, the M.Sc. and Ph.D. degrees in Computer Science from the University of Paris VI, Paris, France, in 1999 and 2003, respectively, and the habilitation degree from the University of Tunis (ISG-Campus) in 2011. He was a Research Fellow with the France Telecom, Research and Development Department, Paris, for three years. He is currently a Full Professor and the Dean of the University of Tunis (ISG-Campus), where he is also the Head of the SMART Laboratory. He published over 110 research papers in refereed international journals, conference proceedings, and book series. His current research interests include multiagent simulation, multicriteria decision making, evolutionary computation, supply chain management, and behavioral economics. He is a reviewer for several artificial intelligence journals and conferences. He can be contacted at email: lamjed.bensaid@isg.rnu.tn.